Progress In Electromagnetics Research Letters, Vol. 4, 9–16, 2008

FRACTAL-LIKE SQUARE LATTICES OF AIR HOLES

H. T. Hattori

Department of Electronic Materials Engineering
Research School of Physical Sciences and Engineering
The Australian National University
Canberra Australia ACT 0200

Abstract—Fractal structures have been widely used in many fields of science, such as biology, physics and chemistry. In this article, we analyze the basic properties of a fractal-like square lattice of air holes, with most of the holes having a lattice constant of Λ while others are repeated with a lattice constant of 2Λ. We change the radii of these holes and analyze their effects on the bandgap regions and transmission properties.

The analysis conducted here is based upon band diagrams and 2D Finite difference time-domain (FDTD) solution of the full-wave Maxwell's equations. We show that this structure provides flexibility in tuning the bandgap of the photonic crystal structure and we show the appearance of mini-bandgap regions along certain directions.

1. INTRODUCTION

Photonic crystals, periodic structures of high index contrast, exhibit the property of forbidding the propagation of light in a certain wavelength range and in certain directions [1]. Photonic crystals offer a unique opportunity to fabricate compact devices because of their ability to confine light in small regions. Moreover, by introducing defects, it becomes possible to create optical waveguides and cavities in the microscale and nanoscale ranges. In fact, photonic crystals have been used in many device applications such as optical fibers [2–4], filters [5–7], waveguide bends [8, 9], magneto-optical devices [10] and lasers [11–14].

"Fractals" is a word used to describe objects that are too irregu ar to be ana yzed by conventional geometry. In other words, sets and functions that are not smooth or regu ar enough compose fractals. They can sometimes represent natura phenomena better than do

conventiona geometric objects [15]. These special geometrical forms have a so been applied to optica devices [16–19], eading to DFB asers with improved performance [18, 19]. Also, fractals have been applied to antennas to produce specially tailored radiation beams [20].

In this article, we combine fractals and photonic crystals and analyze a fractal-like square lattice of air holes. Basically, we merge a set of holes with radius r_1 and lattice constant Λ with another set of holes with radius r_2 and lattice constant 2Λ. Without loss of generality, it is assumed that $r_1 = 0.4\Lambda$. We show that we can tailor the bandgap by changing r_2, even eliminating the bandgap regions for certain values of r_2. Also, min-bandgaps are created along certain directions. Simulations are based upon commercial software: BandSolve to obtain the band diagrams for these structures and Fullwave to provide Finite-Difference Time-Domain Method for these structures.

2. BAND DIAGRAMS OF FRACTAL-LIKE SQUARE LATTICES OF AIR HOLES (FLSL)

The modified square lattice of air holes is shown in Figure 1(a). It consists of a square lattice of air holes with a radius r_1 and lattice constant Λ, surrounding another set of holes organized in a square lattice of air holes with radius r_2 and lattice constant 2Λ. The elementary cell for this structure is shown in Figure 1(b).

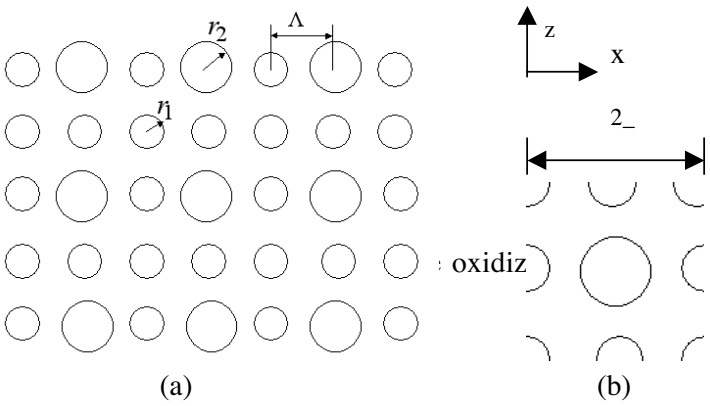

Figure 1. (a) Fractal-like square lattice of air holes (b) Elementary cell for this structure.

The propagating mode is assumed to be TE, with the main magnetic field in the y-direction (perpendicular to the plane containing the photonic crystal structure). The epitaxially layered structure

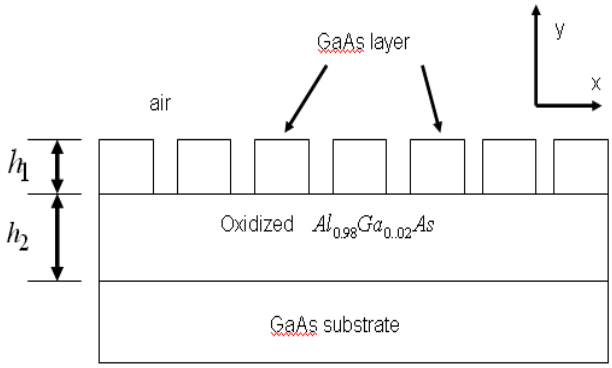

Figure 2. Cross sectional view of the epi-layered structure.

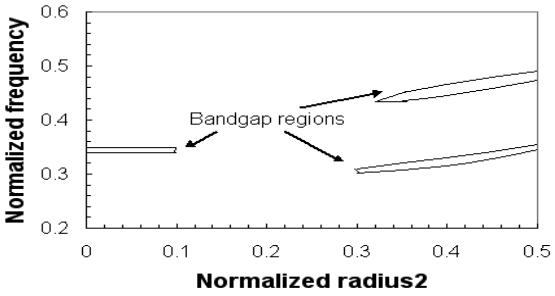

Figure 3. Bandgap regions as a function of normalized radius2 (r_2/Λ).

consists of a GaAs core region (thickness of 140 nm) surrounded by air on top and an oxidized $Al_{0.98}Ga_{0.02}As$ region on the bottom [17], as shown in Figure 2. The thickness of the active region is $h_1 = 140$ nm, while the thickness of the oxidized region (before oxidation) is $h_2 = 450$ nm. For TE modes, this epi-layered structure has an effective index of 2.82.

By using commercial software (BandSolve) [18], we obtain the band diagrams for these structures by solving the equation below,

$$\nabla X \frac{1}{\varepsilon(x,z)} \nabla X \vec{H} = \left(\frac{2\pi}{\lambda}\right)^2 \vec{H} \tag{1}$$

where $\varepsilon(x,z)$ is the electric permittivity function, H is the total magnetic field and λ is the free-space wavelength.

Figure 3 shows the bandgap regions as a function of the normalized radius2 (r_2/Λ). The normalized frequency is expressed in units of

Λ/λ. If $r_2/\Lambda < 0.1$, there is only one bandgap region. Between $0.1 < r_2/\Lambda < 0.28$, the structure presents no bandgap region and, for $0.28 < r_2/\Lambda < 0.52$, the structure presents two bandgap regions. It is clear that, by changing r_2/Λ, we can change the bandgap regions. The argest bandgap region (bandgap extending over the argest frequency range)occurs when $r_2 = 0.4\Lambda$, i.e., when the FLSL collapses into a simple square lattice of air holes.

It should be mentioned that these bandgap regions forbid the propagation of light in a in-plane directions ($\Gamma X, \Gamma M$ and XM directions). There may be mini-bandgaps in certain directions (ΓX direction, for example), as wil be commented ater. The superposition of two photonic crysta s in the same structure can result in the overlapping of the modes from the two photonic crysta s present in the structure or creation of new modes which are generated by the coupling of the modes in these structures. This may explain why certain va ues of r_2 result in no bandgap regions for the FLSL.

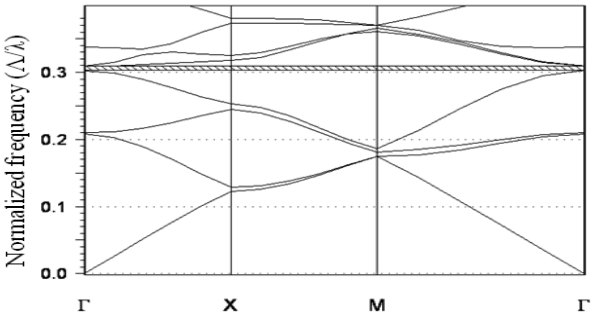

Figure 4. Band diagram for $r_1 = 0.4\Lambda$ and $r_2 = 0.3\Lambda$.

Figure 4 shows a band diagram for $r_1 = 0.4\Lambda$ and $r_2 = 0.3\Lambda$. It is clear that there is a bandgap region between $0.302 < \Lambda/\lambda < 0.309$ in all in-plane directions. There are also "additional" mini-bandgaps along certain directions ($\Gamma X, \Gamma M$ or XM directions). For example, there are mini-bandgaps at $0.1203 < \Lambda/\lambda < 0.1276$ and $0.4304 < \Lambda/\lambda < 0.4364$ along the ΓX direction.

3. FDTD SIMULATIONS OF FRACTAL-LIKE SQUARE LATTICES OF AIR HOLES

In order to assess the in-plane transmission properties of the photonic crystal structures, we employ two-dimensional finite-difference time-domain (FDTD) methods. Commercial software (Fullwave from RSOFT company [19]) is employed. Perfect absorbing layers are placed

at the borders of the computation area. A Gaussian beam covering the photonic crystal region is used as a source to assess the transmission properties of the photonic crystals. A power detector is placed behind the photonic crystal region to assess the transmission spectrum of the photonic crystal structures. The spatial step size of the FDTD simulations is about 40 nm, while the time step is chosen to provide stable FDTD calculations. Without loss of generality, $\Lambda = 300\,\text{nm}$, which provides a bandgap close to $\lambda = 1000\,\text{nm}$, which is the typical operation wavelength of our devices. Light is launched along the ΓX direction, i.e., along the $+z$ direction (see Figure 5(a) for details).

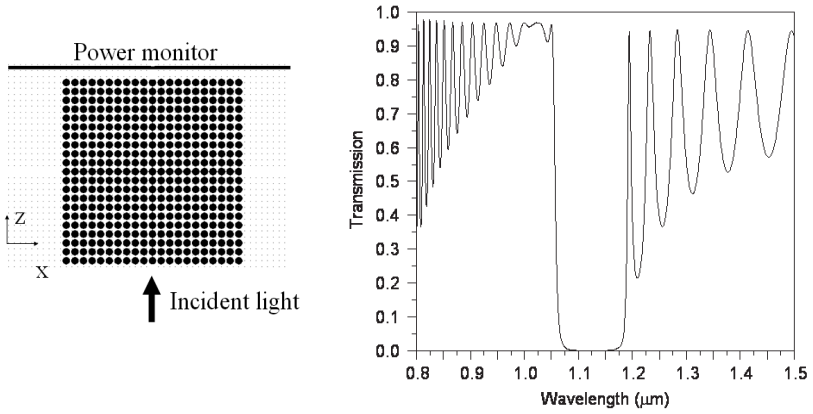

(a) (b)

Figure 5. (a) Basic configuration to assess the transmission properties of photonic crystals (b) Transmission of a square lattice of air holes.

Figure 5(b) shows the transmission spectrum of a square lattice of air holes with $r_1 = r_2 = 120\,\text{nm}$ and $\Lambda = 300\,\text{nm}$. There is a bandgap region between 1075 nm and 1175 nm (the bandgap region occurs when the transmission of light through the photonic crysta is close to zero, i.e., light is not allowed to propagate in the photonic crystal), corresponding to a bandgap in the region $0.26 < \Lambda/\lambda < 0.28$. The band diagrams indicated a bandgap in the region $0.317 < \Lambda/\lambda < 0.327$. One major cause of discrepancies includes the finite number of holes in the FDTD simulations (occupying an area of $6\,\mu$m by $6\,\mu$m, approximately), while band diagrams assume an infinite structure. Also, bandSolve the magnetic field is expanded into a set of plane waves, while in FDTD simulations, the source has a finite spot-size diameter (about $4\,\mu$m). No mini-gaps were observed for this structure in the ΓX direction.

Now, let us assume that $r_1 = 120\,\text{nm}$, $r_2 = 90\,\text{nm}$ and $\Lambda = 300\,\text{nm}$.

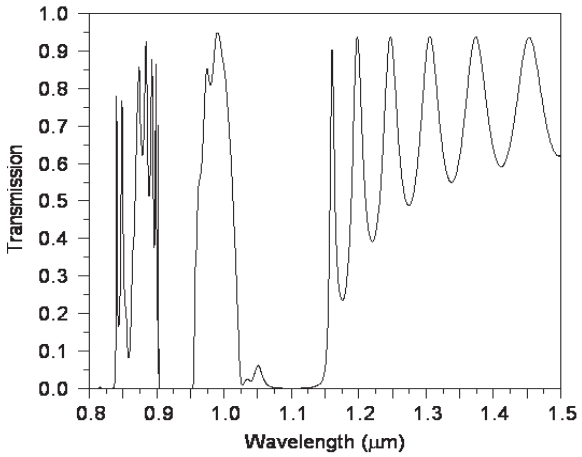

Figure 6. Transmission of a fractal-like structure with $r_1 = 120\,\text{nm}$, $r_2 = 90\,\text{nm}$ and $\Lambda = 300\,\text{nm}$.

The transmission along the ΓX direction is shown in Figure 6.

The bandgap region has shifted to $1050\,\text{nm} < \lambda < 1150\,\text{nm}$ and it is also clear the presence of the mini-gaps along the ΓX directions. These mini-gaps in certain directions may be an additional feature of the FLSL. It should be mentioned that these mini-bandgaps occur for lower wave engths (i.e., wavelengths lower than $1\,\mu\text{m}$), mini-bandgaps at longer wave engths were not noted with the FDTD simulations. At longer wavelengths, the FLSL allows the transmission of light through this structure, as can be clearly observed in Figure 6 (the structure is in the valence band, where there are many modes that can propagate in this structure).

FLSL gives an additional degree of freedom to control the position of the bandgap regions and generate mini-bandgaps in certain directions. These features may lead to new applications to optica devices in the future.

4. CONCLUSIONS

In this article, we presented the basic properties of fractal-like square lattices of air holes. We showed that the bandgap region can be tailored in these structures and mini-bandgaps along certain directions (e.g., ΓX) appear in these structures.

ACKNOWLEDGMENT

The author gratefully acknow edges the financial support from the Australian Research Council (ARC) to realize this work.

REFERENCES

1. John, S., "Strong localization of photons in certain disordered dielectric superlattices," *Physical Review Letters*, Vol. 58, 2486–2489, 1987.
2. Knight, J. C., T. A. Birks, P. St J. Russell, and D. M. Atkins, "Pure silica single-mode fiber with hexagonal photonic crystal cladding," *Optics Letters*, Vol. 21, 1547–1549, 1996.
3. Schneider, V. M. and H. T. Hattori, "Dispersion characteristics of segmented optical fibers," *Applied Optics*, Vol. 44, 2391–2395, 2005.
4. Franco, M. A. R., E. C. S. Barreto, V. A. Serrao, F. Sircilli, and H. T. Hattori, "Analysis of highly birefringent photonic crystal fibers with squeezed rectangular lattices," *Microwave and Optical Technology Letters*, Vol. 50, 1083–1086, 2008.
5. Fan, S., P. R. Villeneuve, and J. D. Joannopoulos, "Channel drop filters in photonic crystals," *Optics Express*, Vol. 3, 4–11, 1998.
6. Matsumoto, T. and T. Baba, "Photonic crystal k-vector superprism," *Journal of Lightwave Technology*, Vol. 22, 917–922, 2004.
7. Chen, C., B. Miao, and D. Prather, "Tunable photonic crystal based on SOI," *PIERS Online*, Vol. 2, 574–578, 2007.
8. Fan, S., S. G. Johnson, J. D. Joannopoulos, C. Manolatou, and H. A. Haus, "Waveguide branches in photonic crystals," *Journal of the Optical Society of America B*, Vol. 18, 162–165, 2001.
9. Tayeboun, F., R. Naoum, H. M. Tayeboun, H. T. Hattori, and F. Salah-Belkhodja, "Improved transmission waveguide bends in photonic crystal," *Journal of Electromagnetic Waves and Applications*, Vol. 19, 615–628, 2005.
10. Dimitriev, V., "2D magnetic photonic crystals with square lattice-group theoretical standpoint," *Progress In Electromagnetics Research*, PIER 68, 71–100, 2006.
11. Hattori, H. T., V. M. Schneider, R. M. Cazo, and C. L. Barbosa, "Analysis of strategies to improve the directionality of square lattice band-edge photonic crystal structures," *Applied Optics*, Vol. 44, 3069–3076, 2005.
12. Hattori, H. T., I. Mc Kerracher, H. H. Tan, and C. Jagadish, "In-

plane coupling of light from InP-based photonic crystal band-edge lasers into single-mode waveguides," *IEEE Journal of Quantum Electronics*, Vol. 43, 279–286, 2007.

13. Painter, O., R. K. Lee, A. Scherrer, A. Yariv, J. D. O'Brien, P. D. Dapkus, and I. Kim, "Two-dimensional photonic band-gap defect mode laser," *Science*, Vol. 284, 1819–1821, 1999.
14. Ohnishi, D., T. Okano, M. Imada, and S. Noda, "Room temperature continuous wave operation of a surface-emitting two-dimensional photonic crystal diode laser," *Optics Express*, Vol. 12, 1562–1568, 2004.
15. Barnsley, M., *Fractals Everywhere*, Academic, Boston, 1988.
16. Hattori, H. T., V. M. Schneider, C. L. Barbosa, and R. M. Cazo, "Reflectivity spectra evolution in grating structures with fractionally organized gaps," *Microwave and Optical Technology Letters*, Vol. 29, 42–45, 2001.
17. Barbosa, C. L., R. M. Cazo, and H. T. Hattori, "Grating structures with symmetric fractionally organized gaps," *Microwave and Optical Technology Letters*, Vol. 31, 223–229, 2001.
18. Hattori, H. T., V. M. Schneider, and C. L. Barbosa, "Analysis of distributed-feedback lasers with fractionally organized gaps," *Applied Optics*, Vol. 46, 1283–1289, 2007.
19. Hattori, H. T., H. H. Tan, and C. Jagadish, "Analysis of optically pumped compact laterally coupled distributed feedback lasers with three symmetric defect regions," *Journal of Applied Physics*, Vol. 102, 083109 1-8, 2007.
20. Biswas, B. N., R. Ghatak, R. K. Mishra, and D. R. Poddar, "Characterization of a self-complementary Sierpinski Gasket microstrip antennas," *PIERS Online*, Vol. 2, 698–701, 2006.
21. BandSolve 2.0 RSOFT design group, 1999.
22. Fullwave 7.0 RSOFT design group, 2007.